

# The Phenomenon of High Hardness Values on the S-Phase Layer of Austenitic Stainless Steel via Screen Plasma Nitriding Process

Sang-Gweon Kim<sup>1</sup>, Kook-Hyun Yeo<sup>1</sup>, Yong-Ki Cho<sup>1</sup>, Jae-Hoon Lee<sup>1</sup>, Masahiro Okumiya<sup>2</sup>

<sup>1</sup>Heat Treatment R&D Group, Korea Institute of Industrial Technology (KITECH), Siheung, Republic of Korea

<sup>2</sup>Toyota Technological Institute, Nagoya, Japan

Email: kimsg@kitech.re.kr

**How to cite this paper:** Kim, S.-G., Yeo, K.-H., Cho, Y.-K., Lee, J.-H. and Okumiya, M. (2018) The Phenomenon of High Hardness Values on the S-Phase Layer of Austenitic Stainless Steel via Screen Plasma Nitriding Process. *Advances in Materials Physics and Chemistry*, 8, 257-268.  
<https://doi.org/10.4236/ampc.2018.86017>

**Received:** May 2, 2018

**Accepted:** June 26, 2018

**Published:** June 29, 2018

Copyright © 2018 by authors and Scientific Research Publishing Inc.

This work is licensed under the Creative Commons Attribution International License (CC BY 4.0).

<http://creativecommons.org/licenses/by/4.0/>



Open Access

## Abstract

The purpose of this study is to improve the surface properties of austenitic stainless steel using the double-folded electrode screen plasma nitriding (SPN) process. In general, the S-phase is well-known for its excellent properties such as improved hardness and wear resistance along with sustained corrosion resistance. The concentrated nitrogen via SPN process was injected to form S-phase with time at 713 K. This study was carried out under the conditions of 44 at% of nitrogen injection, which was higher than 25 at% known as the condition of no precipitation of S-phase formed by the SPN process, and 20 K higher than the maximum temperature without precipitation phase. The hardness analysis of stainless steel sample treated by the SPN process at 713 K showed a much higher value than the typical nitriding hardness at a depth of lower nitrogen than the maximum nitrogen concentration. The SPN 20 hr treated specimen showed the average value of 2339 HV while 40 hr showed the average value of 2215 HV. The result is attributed to the concentrated nitrogen formed in the SPN process reacting with the alloying elements contained in the base material to form fine precipitates, thus producing a synergy effect of the extreme hardening effect; that is, the movement of precipitates and dislocations due to the GP-zone (Guinier-Preston zone).

## Keywords

Double-Folded Electrode, Austenitic Stainless Steel (ASS), Screen Plasma Nitriding (SPN) Process, S-Phase, Corrosion Resistance, High Hardness

## 1. Introduction

The double-folded electrode Screen Plasma Nitriding (SPN) process of austenitic

stainless steel (ASS) at low temperatures has been extensively studied to understand the factors influencing the formation of nitrogen expanded austenite (S-phase) [1] [2] [3] [4] [5]. The S-phase provides high hardness and wear-resistance, and for this reason, there are potential demands for S-phase from the industries of machinery, mold tools and automotive parts [4].

The S-phase on the surface of ASS is thermodynamically unstable when it is oversaturated with interstitial atoms such as nitrogen and carbon. This is because the state of oversaturation induces internal stress that distorts lattice and increases the volume of ASS [6].

The residual stress, or internal stress, of ASS leads to the formation of CrN-precipitates after nitriding, which results in severe corrosion through the formation of galvanic cells [7]. Also, the formation of cracks can initiate from the locations with high composition-induced stress in ASS.

Christiansen suggested that high nitrogen potential is located near the surface of the S-phase, which leads to the push-out of grain for relaxing the stress. This implies that corrosion can initiate at the locations where grain push-out occurs [8]. Indeed, the phenomena of corrosion were observed in the S-phase when the sample was immersed in an acid mixture of 50% HCl/H<sub>2</sub>SO<sub>4</sub> (3:1) and 50% H<sub>2</sub>O, as shown in **Figure 1**.

Christiansen *et al.* also proposed a corrosion model based on the simulation for the relationship between the amount of nitrogen diffused into the matter and the distribution of residual stress during gas nitriding process [8]. He also mentioned that the formation of cracks is likely to occur above 25 at% of the amount

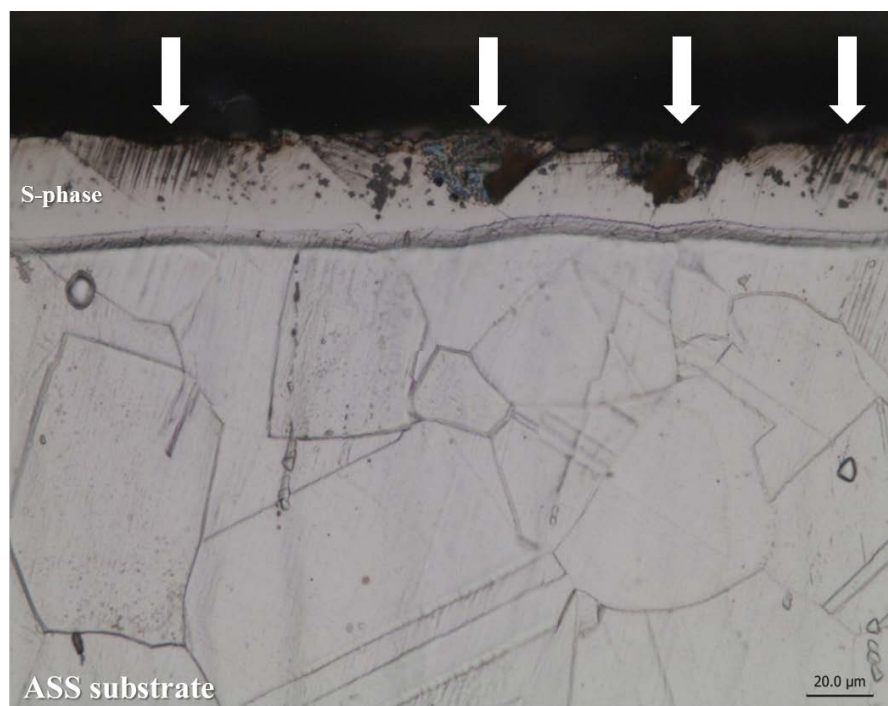


**Figure 1.** Corrosion of the S-phase after immersed in an acid mixture (50% HCl/H<sub>2</sub>SO<sub>4</sub> (3:1) and 50% H<sub>2</sub>O). The location after corrosion test is indicated by a white arrow.

of nitrogen atoms in the S-phase.

Kim *et al.* referred to the principle of high density nitrogen generation by screen plasma technology and reported a very high nitrogen concentration compared to other nitriding processes at a nitrogen concentration of 44 at% and a temperature of 713 K [9].

This study reports the result showing the particularly high hardness even when considering that the error range is high since the micro hardness is very large during the process of controlling the phase formation through aging by slow cooling after injecting concentrated nitrogen in the precipitation zone of S-phase for the study of the formation of more hardened surface despite the loss of nitride layer by precipitate.

## 2. Experimental Procedures

Disc samples of ASS with the size of 10 mm by 30 mm were prepared. The nominal composition of the ASS (AISI 316L or JIS-SUS316L) was 0.03% C, 2% Mn, 0.75% Si, 0.045% P, 0.03% S, 16% - 18% Cr, 10% - 14% Ni, and 0.1% N (**Table 1**).

The bright polished ASS was treated using a SPN equipment (**Figure 2**) as follows. The samples were placed in a double-folded screen electrode set-up on the electrically insulated plate (cathode) surrounded by the chamber wall (anode). The double-folded screen electrode was a mesh cylinder of 700 mm in

**Table 1.** Chemical composition of AISI 316L (ASS) used in the experiments (%).

Chemical composition	C	Cr	Mn	N	Ni	P	S	Si
AISI316L (ASS)	0.03	16.0 - 18.0	2.0	0.1	10.0 - 14.0	0.045	0.03	0.75

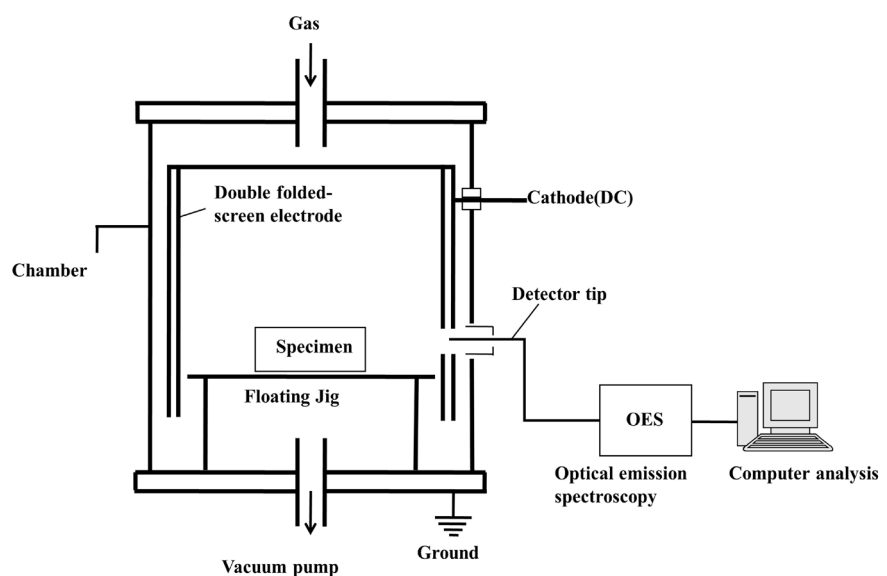


**Figure 2.** Illustration of the SPN set-up.

diameter and was 900 mm high with a 1 mm perforated AISI 304 steel sheet. During the SPN processing, DC power (maximum output: 600 V/50A) was applied to the double-folded screen electrode to increase the temperature. The processing temperatures for SPN process were 713 K, respectively, at fixed 0.15 Torr for 4, 10, 20, and 40 hours. During the process, N<sub>2</sub>/H<sub>2</sub> gas with gas ratio of 1 to 3 were used with 320 sccm.

The microstructure of the samples after SPN treated sample was observed using SEM/EDS (FEI Hong Kong Company, NNS-450 and Bruker LN2 free SDD EDS). XRD data were collected using a PANalytical X-ray diffractometer with Cu K $\alpha$  radiation ( $\lambda = 1.5405 \text{ \AA}$ ) for the investigation of phase composition. Hardness and depth profile of the samples were measured using a micro-Vickers hardness tester (Matsuzawa, MMT-3).

### 3. Results and Discussion

The SPN process enables the diffusion of a high concentration of nitrogen atoms into ASS at relatively low temperatures compared to other nitriding processes such as gas nitriding. The effectiveness of double-folded screen electrode in plasma nitriding is attributed to the ease of diffusion with smaller size of active nitrogen species such as neutral nitrogen (N), NH<sub>x</sub>, N<sub>2</sub><sup>\*</sup> and N<sub>2</sub><sup>+</sup> generated by plasma nitriding. The concentration of nitrogen atoms is one of the main variables that determine the diffusion depth according to Fick's law. Also, the temperature as a processing parameter is the driving force for diffusion of nitrogen atoms into the ASS substrate. For example, diffusion depth of the nitrogen atoms is determined by the temperature during the nitriding process [9] [10].

**Figure 3** shows the cross section images of samples treated with the SPN process at the temperature of 713 K for (a) 8  $\mu\text{m}$  thickness at 4, (b) 14  $\mu\text{m}$  thickness at 10, (c) 21  $\mu\text{m}$  thickness at 20, and (d) 40  $\mu\text{m}$  thickness at 40 hours. The thickness of formed nitride layer and formation and growth of crack on the surface increased proportionally to the screen plasma nitriding duration. **Figure 3** (a) shows the formation of the layer without crack while **Figure 3(b)** shows the beginning of some cracks. **Figure 3(c)** shows the formation of new phase from the outer part while **Figure 3(d)** shows the large spread of the new phase (Cr<sub>x</sub>N<sub>1-x</sub> precipitated phase) throughout the nitrided layer.

It is well established that a higher nitriding potential induced by higher temperature causes brittleness to the S-phase, which is associated with high stress induced by composition, a high yield stress and limited ductility [8] [9].

X-ray diffraction patterns of the ASS samples at different processing steps are shown in **Figure 4**. Diffraction patterns of FCC iron structure were observed indicating the status of the non-treated ASS.

The crystallographic data of the nitrided ASS provide information including phase identity as well as lattice strain induced by internal stress. The diffusion of nitrogen atoms into the octahedral interstitials of the ASS substrate leads to the

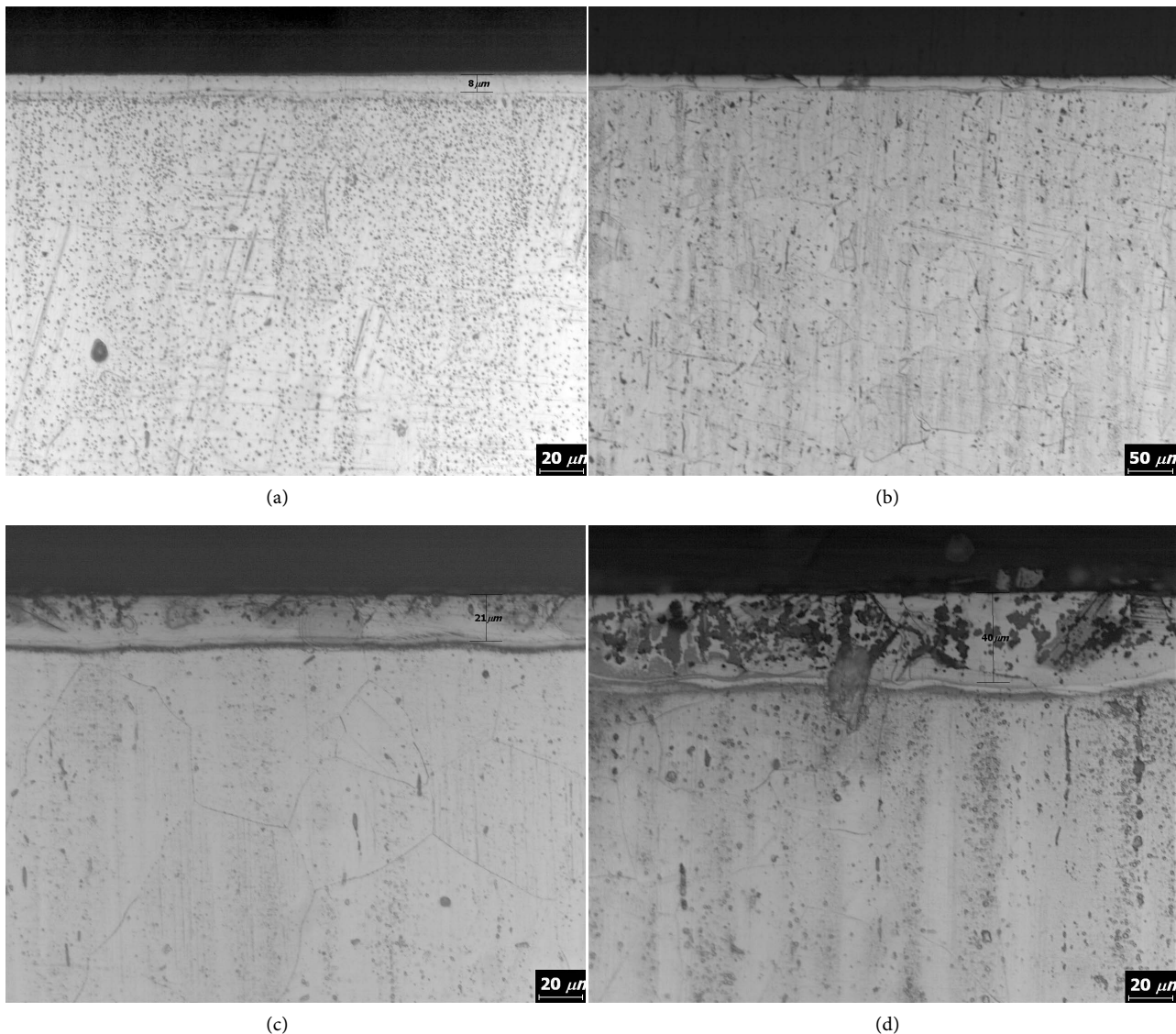


**Figure 3.** Cross section images of the SPN treated ASS with different time at (a) 4, (b) 10, (c) 20, and (d) 40 hours.

expansion of unit cells in the S-phase during the nitriding process different times. In addition to this, the fault (*i.e.* stacking fault) of the face centered cubic (FCC) lattice causes  $2\theta$  peak shift to the nitrided ASS, compared to the bare ASS [11] [12].

For the S-phase prepared at 713 K, peak shift to the lower  $2\theta$  angle as well as peak broadening with different diffusion concentration, about  $3^\circ$  and over, are clearly shown, which imply that the unit cell volume expands due to the larger amount of nitriding-induced nitrogen interstitials in the S-phase [8].

Comparison of ASS raw material and X-ray peak by the SPN process as shown in **Figure 4** indicates the formation of S-phase in the maximum grid constant after the sample is treated for 4 hours or longer. However, it also shows the peak becoming wider as it moves to the right again at 713 K and 20 hr, leading to the precipitation of nitride with epsilon phase ( $\epsilon$ -Fe<sub>2-3</sub>N) as the nitrogen leaves the

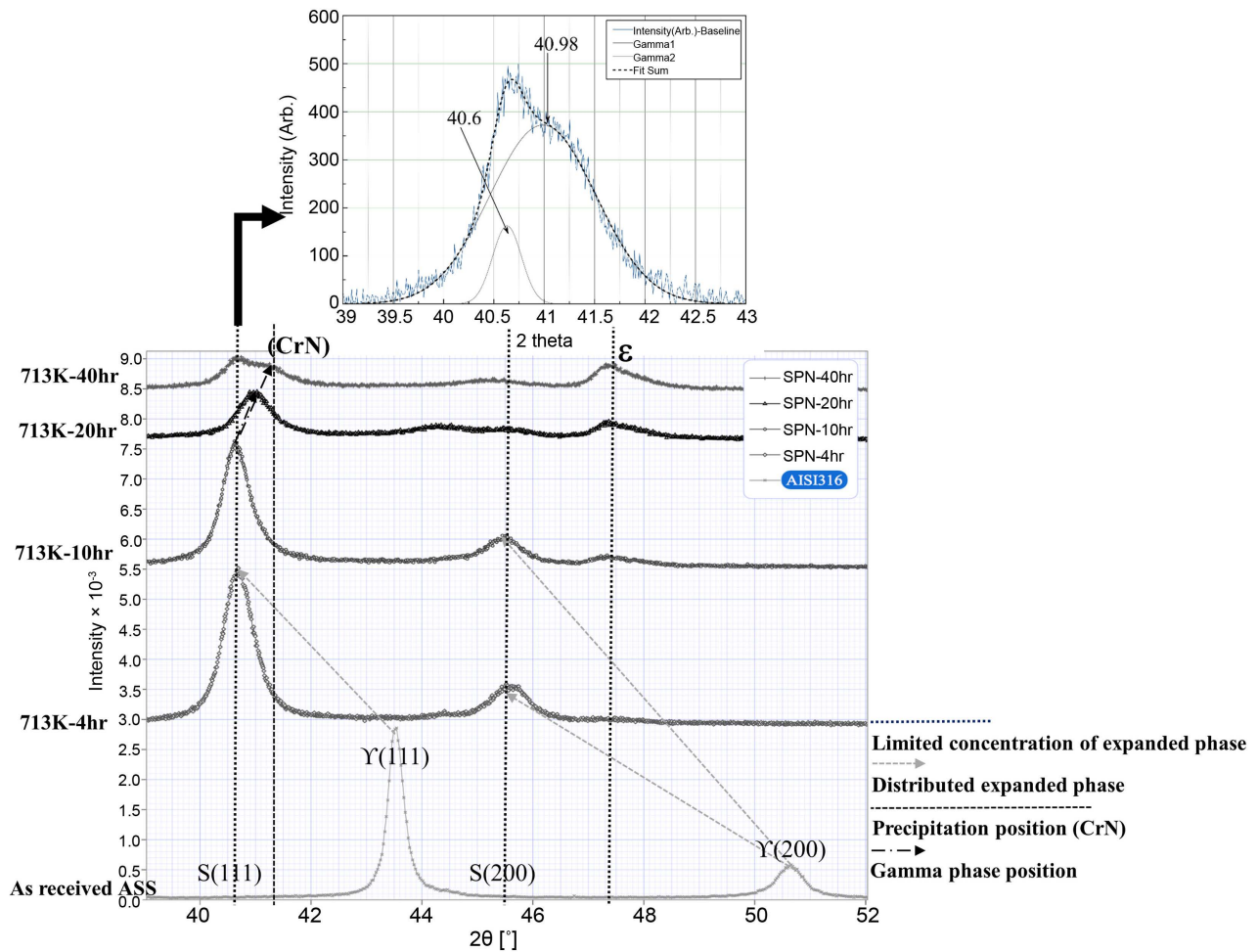
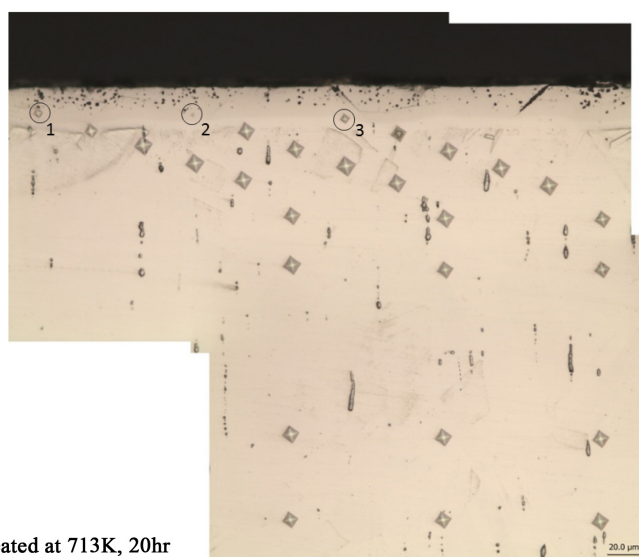
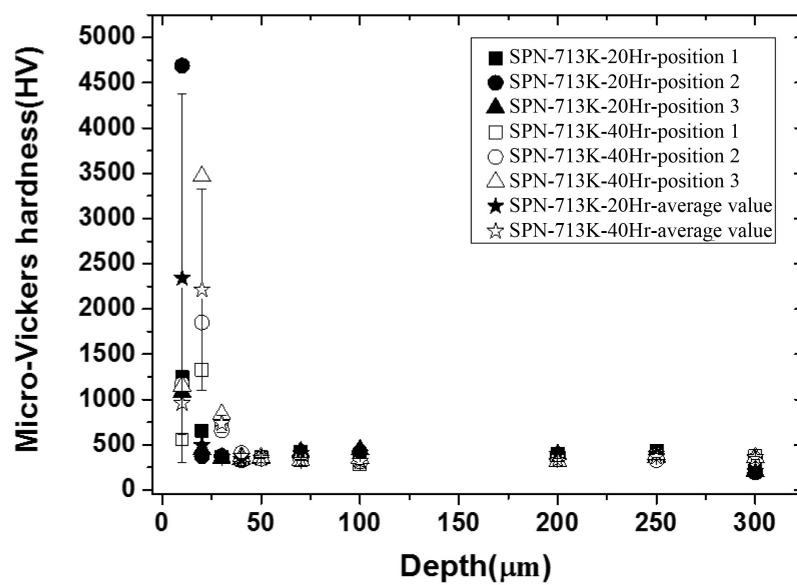


**Figure 4.** X-ray diffraction patterns of SPN treated layer at 713 K as functions of the treatment time.

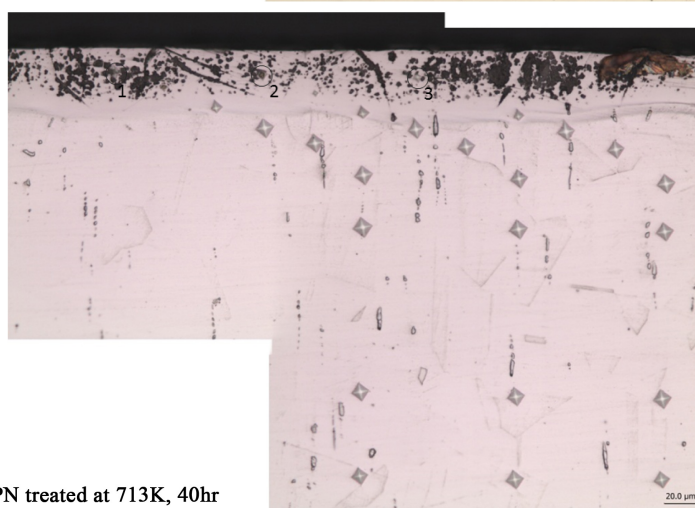
grid. At 713 K and 40 hr, the peak is separated into two or more as shown in **Figure 4**. Such phenomenon confirms the fact that the change of tissue according to the nitriding time as shown in the images of cross section image with time in figure matches the change of X-ray peak according to the screen plasma nitriding time. And the longer the screen plasma nitriding time, the wider the X-ray peaks, which indicate finer grain size. The fine grain size is expected to contribute to the increased strength and hardness of the alloy.

The distribution of hardness profile along the depth of the S-phase on ASS after SPN processing is depicted in **Figure 5**. Although the figure shows the typical hardness value of about 1300 HV<sub>0.025</sub> in the layer where the S-phase contains CrN precipitation, the maximum hardness was observed in positions where the nitrogen concentration was not particularly high. To explain such high hardness, P. A. Dearnley [5] and T. Christiansen [13] reported the maximum hardness of about 20 GPa when the nitrogen content in the S-phase was of 8 and maximum of about 30 at% and then a lower value with the additional precipitation of phase.

On the other hand, X. Y. Li *et al.* analyzed the phase with X-TEM and reported



SPN treated at 713K, 20hr



SPN treated at 713K, 40hr

**Figure 5.** Hardness-depth profile of the nitriding layers via SPN on the ASS prepared at 713 K for 20 hr and 40 hr.

that the difficulty of dislocation in the S-phase increased the hardness and the hardness increased to an extreme level by increase of phases (mostly  $\gamma'$ -M<sub>4</sub>N, M = Cr, Fe, and Mo etc.) precipitated in the sublayer, that is the phase [14].

The study of phase distribution showed the difference of precipitation phase according to depth. However, the phenomenon must be analyzed with the phase structure and thus is excluded from this study.

**Figure 6** shows the results of the line scanning and mapping according location-specific EDS. **Figure 6(a)** shows the compositional at positions 1 through 4 at each depth of the layer, and **Figure 6(b)** shows the result of S-phase component analysis with line scanning and indicates the similar component distribution at each depth. **Figure 6(c)** shows the result of EDS mapping of the S-phase layer and indicates that the stains on the S-phase are in the form of Cr and Mo nitrides.

Diffusion profile of the nitrogen atoms in the ASS is closely related with the concentration-dependent diffusivity of nitrogen atoms along the depth of the S-phase. The nitrogen potentials are reflected in the atomic concentration-depth profile of the nitrated layer on ASS as shown in **Figure 7**.

In **Figure 7**, the atomic concentration of nitrogen near the surface of S-phase is 44 at% which implies that the nitrogen contents at the surface increase during the SPN 20 hours treatment. Particularly, a steep increase of the nitrogen concentration towards the surface of the S-phase after the smooth increase of the nitrogen gradient from the ASS substrate was observed on the sample.

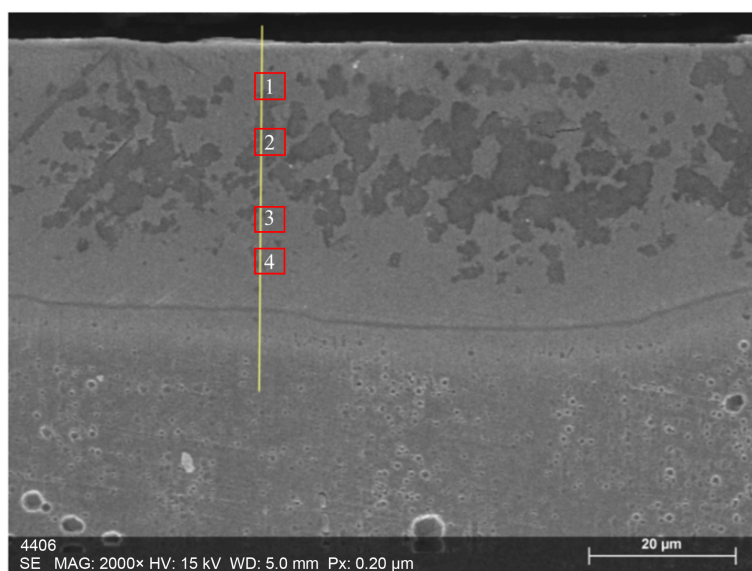
Interestingly, a very small amount of carbon atoms was observed at the location where diffusion of nitrogen atoms towards the ASS substrate halts, as shown in the insets of the **Figure 5**, which implies that carbon atoms in bare ASS are pushed ahead by the diffusion of nitrogen atoms during screen plasma nitriding procedure.

Comparison of the gradient of nitrogen concentration in **Figure 7** and the images of 713 K for 20 hr and observed hardness in **Figure 5** indicates that the nitrogen concentration showing the maximum hardness is at 20 at%, not 44 at%.

## 4. Conclusions

The S-phase of the ASS was prepared using SPN treatment at different times. The prior studies have focused on decreasing deterioration of corrosion resistance due to a formation of S-phase. However, increasing the process time of S-phase will result in precipitation of new phase in the S-phase by the CrN and the contents in ASS.

The SPN treatment of sample at the temperature of 713 K for 4 hours showed no precipitation phase or crack initially and then the fine cracks beginning to form after 10 hours and the precipitation phase observed in the S-phase at 20 hours. The precipitation phase spread throughout the whole S-phase after 40 hours. The result showed that the phase-forming behavior agreed well with the peak shift and the phase separation phenomenon of the X-ray diffraction pattern.



Name	Date	Time	HV [kV]	Mag	WD [mm]
4406	5/23/2017	4:39:11 PM	15.0 keV	2000x	5.0 mm

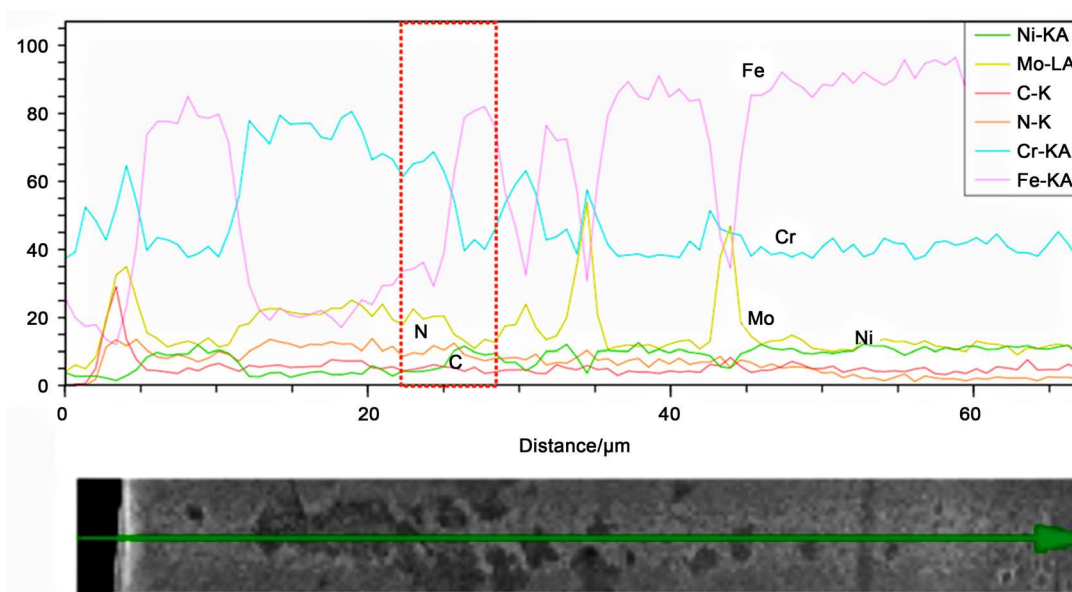
Element	At. No.	Line s.	Mass [%]	Mass Norm. [%]	Atom [%]	abs. error [%] (1 sigma)
Carbon	6	K-Serie	2.79	3.08	10.44	0.80
Nitrogen	7	K-Serie	4.82	5.33	15.49	1.10
Oxygen	8	K-Serie	2.99	3.31	8.41	0.65
Sulfur	16	K-Serie	0.94	1.04	1.32	0.07
Chromium	24	K-Serie	17.34	19.17	15.00	0.57
Manganese	25	K-Serie	1.58	1.74	1.29	0.11
Iron	26	K-Serie	51.99	57.45	41.88	1.62
Nickel	28	K-Serie	8.03	8.88	6.16	0.37
			<b>90.50</b>	<b>100.00</b>	<b>100.00</b>	

Element	At. No.	Line s.	Mass [%]	Mass Norm. [%]	Atom [%]	abs. error [%] (1 sigma)
Carbon	6	K-Serie	3.36	3.85	12.18	0.91
Nitrogen	7	K-Serie	5.65	6.49	17.59	1.24
Oxygen	8	K-Serie	3.76	4.31	10.24	0.78
Sulfur	16	K-Serie	1.43	1.64	1.95	0.09
Chromium	24	K-Serie	23.12	26.55	19.39	0.74
Manganese	25	K-Serie	2.14	2.45	1.70	0.13
Iron	26	K-Serie	41.71	47.89	32.56	1.33
Nickel	28	K-Serie	5.93	6.81	4.41	0.30
			<b>87.09</b>	<b>100.00</b>	<b>100.00</b>	

Element	At. No.	Line s.	Mass [%]	Mass Norm. [%]	Atom [%]	abs. error [%] (1 sigma)
Carbon	6	K-Serie	2.49	2.83	10.00	0.75
Nitrogen	7	K-Serie	4.29	4.87	14.77	1.01
Oxygen	8	K-Serie	1.55	1.76	4.67	0.41
Sulfur	16	K-Serie	1.12	1.27	1.68	0.08
Chromium	24	K-Serie	19.57	22.20	18.14	0.64
Manganese	25	K-Serie	2.09	2.37	1.84	0.13
Iron	26	K-Serie	49.86	56.57	43.02	1.56
Nickel	28	K-Serie	7.16	8.13	5.88	0.34
			<b>88.14</b>	<b>100.00</b>	<b>100.00</b>	

Element	At. No.	Line s.	Mass [%]	Mass Norm. [%]	Atom [%]	abs. error [%] (1 sigma)
Carbon	6	K-Serie	2.40	2.56	9.63	0.75
Nitrogen	7	K-Serie	3.29	3.50	11.30	0.85
Oxygen	8	K-Serie	0.75	0.79	2.24	0.26
Sulfur	16	K-Serie	0.87	0.93	1.31	0.07
Chromium	24	K-Serie	16.98	18.06	15.72	0.56
Manganese	25	K-Serie	1.80	1.92	1.58	0.12
Iron	26	K-Serie	59.47	63.24	51.26	1.85
Nickel	28	K-Serie	8.48	9.02	6.95	0.39
			<b>94.04</b>	<b>100.00</b>	<b>100.00</b>	

(a)



Name	Date	Time	Points	Length [mm]
Scan data	5/23/2017	4:48:37 PM	100	66.9 μm
	5/23/2017			

(b)

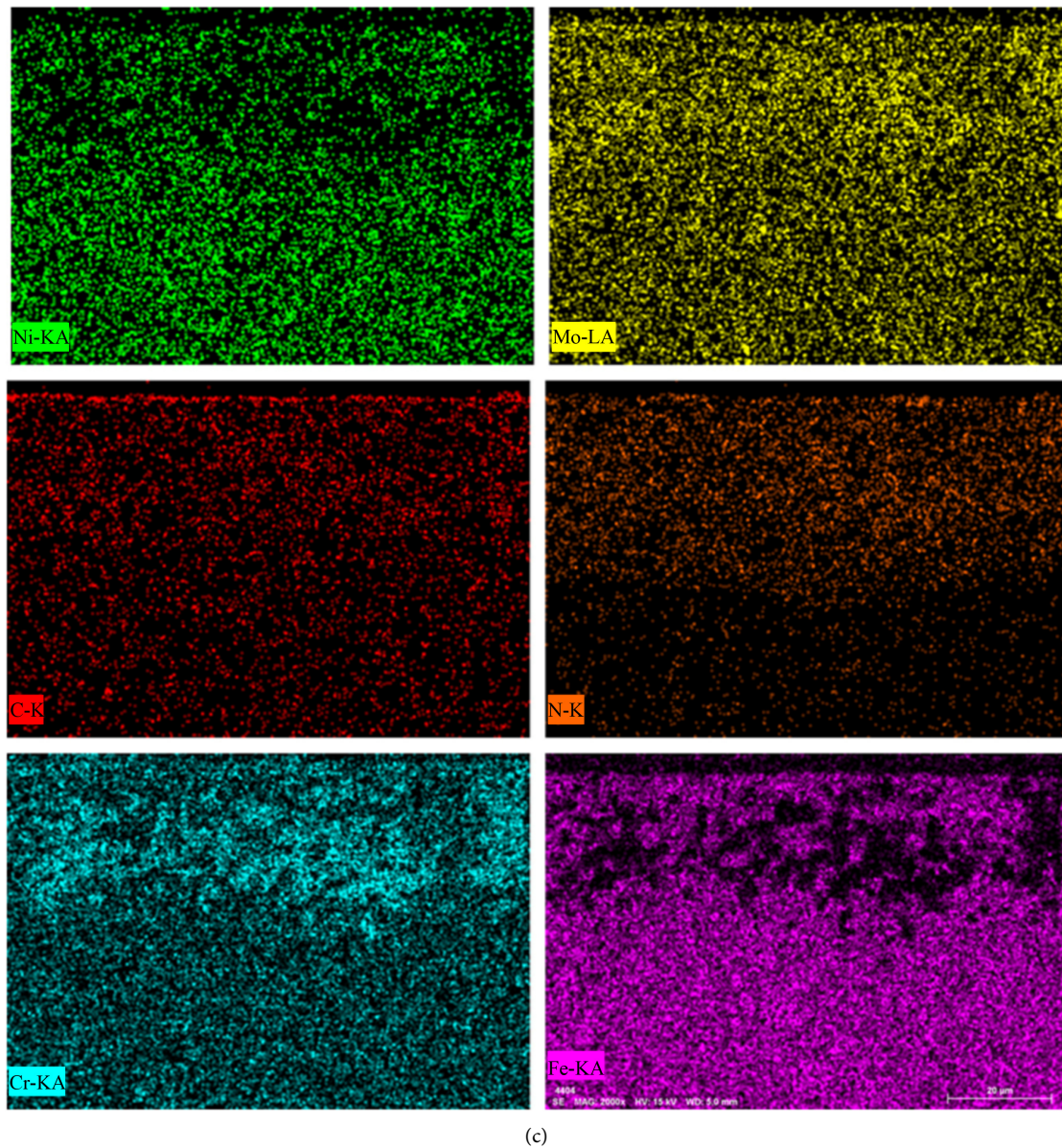


**Figure 6.** Result of line profiling of each position of S-phase layer and mapping of nitride layer using SEM/EDS. (a) Component analysis of 1 - 4 position of S-phase by point scanning. (b) Component analysis of S-phase by line scanning. (c) Component analysis by mapping of S-phase.

On the other hand, the analysis of hardness according to the time of S-phase formation showed a very high hardness value of 4689 HV<sub>0.025</sub> after 20 hours. The value was notable in that it was much higher than the hardness value according to formation of S-phase and that such high hardness value was observed at the position of about 20 at% instead of the maximum nitrogen concentration of 44 at%. We did not find any other precipitation on the position and are currently carrying out an in-depth study.

Under a circumstance, we consider the phenomenon very important because it means the possible development of the layer that shows the maximum hardness of 4689 HV as the result of new precipitation phase in the form of GP-zone

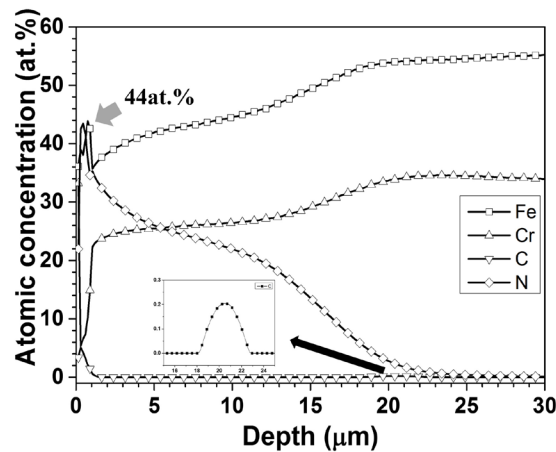


**Figure 7.** Atomic concentration of different atoms (Fe, N, C, and Cr) along the depth of the S-phase layer on the ASS prepared via SPN process at 713 K 20 hr.

by aging and lattice parameter change of nitrogen during cooling.

It suggests the direction for the development of new methods of SPN treatment if a high degree of wear resistance is necessary even if it means some deterioration of corrosion resistance.

## References

- [1] Zhao, C., Li, C.X., Dong, H. and Bell, T. (2006) Study on the Active Screen Plasma nitriding and Its Nitriding Mechanism. *Surface and Coatings Technology*, **201**, 2320. <https://doi.org/10.1016/j.surfcoat.2006.03.045>
- [2] Han, L., Daia, J.T., Huang, X.R. and Zhao, C. (2013) Study on the Fast Nitriding Process of Active Screen Plasma Nitriding. *Physics Procedia*, **50**, 94. <https://doi.org/10.1016/j.phpro.2013.11.017>
- [3] Li, C.X., Georges, J. and Li, X.Y. (2002) Active Screen Plasma Nitriding of Austenitic Stainless Steel. *Surface Engineering*, **18**, 453. <https://doi.org/10.1179/026708402225006240>
- [4] Samandi, M., Shedden, B.A., Smith, D.F.I., Collins, G.A., Hutchings, R. and Tendys, J. (1993) Microstructure, Corrosion and Tribological Behaviour of Plasma Immersion Ion-Implanted Austenitic Stainless Steel. *Surface and Coatings Technology*, **59**, 261. [https://doi.org/10.1016/0257-8972\(93\)90094-5](https://doi.org/10.1016/0257-8972(93)90094-5)
- [5] Dearnley, P.A. (2002) Corrosion Wear Response of S Phase Coated 316L. *Surface Engineering*, **18**, 429. <https://doi.org/10.1179/026708402225006277>
- [6] Zhang, Z.L. and Bell, T. (1985) Structure and Corrosion Resistance of Plasma Nitrided Stainless Steel. *Surface Engineering*, **1**, 131. <https://doi.org/10.1179/sur.1985.1.2.131>
- [7] Schramm, R.E. and Reed, R.P. (1975) Stacking Fault Energies of Seven Commercial Austenitic Stainless Steels. *Metallurgical and Materials Transactions A*, **6A**, 1345. <https://doi.org/10.1007/BF02641927>
- [8] Christiansen, T.L. and Somers, M.A.J. (2009) Low-Temperature Gaseous Surface Hardening of Stainless Steel: The Current Status. *International Journal of Materials Research*, **100**, 1361. <https://doi.org/10.3139/146.110202>
- [9] Kim, S.-G., Lee, J.-H., Saito, N. and Takai, O. (2013) The Role of Activated Nitrogen

Species on Double-Folded Screen Nitriding Process. *Journal of Physics: Conference Series*, **417**, 1. <https://doi.org/10.1088/1742-6596/417/1/012023>

- [10] Yeo, K.-H., Kim, S.-G., Lee, J.-H., Kong, J.-H. and Okumiya, M. (2014) Trend of Nitriding on Chromium-Molybdenum Steel via Low Temperature Screen Plasma Technology. *Advances in Materials Physics and Chemistry*, **4**, 141. <https://doi.org/10.4236/ampc.2014.48017>
- [11] Velterop, L., Delhez, R., de Keijser, Th.H., Mittemeijer, E.J. and Reefman, D. (2000) X-Ray Diffraction Analysis of Stacking and Twin Faults in f.c.c. Metals: A Revision and Allowance for Texture and Non-Uniform Fault Probabilities. *Journal of Applied Crystallography*, **33**, 296. <https://doi.org/10.1107/S0021889800000133>
- [12] Fewell, M.P. and Priest, J.M. (2008) High-Order Diffractometry of Expanded Austenite Using Synchrotron Radiation. *Surface and Coatings Technology*, **202**, 1802. <https://doi.org/10.1107/S0021889800000133>
- [13] Christiansen, T., Dahl, K.V. and Somers, M.A.J. (2008) Nitrogen Diffusion and Nitrogen Depth Profiles in Expanded Austenite: Experimental Assessment, Numerical Simulation and Role of Stress. *Materials Science and Technology*, **24**, 159. <https://doi.org/10.1179/026708307X232901>
- [14] Li, X.Y., Sun, Y., Bloyce, A. and Bell, T. (1997) XTEM Characterisation of Low Temperature Plasma Nitrided AISI 316 Austenitic Stainless Steel. Institute of Physics Conference Series No. 153: Section 13, 633.